Ultrasonics - Sonochemistry 48 (2018) 110–117

Contents lists available at ScienceDirect

Ultrasonics - Sonochemistry

journal homepage: www.elsevier.com/locate/ultson

Sonochemical reduction of Cr(VI) in air in the presence of organic additives: What are the involved mechanistic pathways?

Jorge M. Meichtry[a,b], Mariel Slodowicz[a,b], Lucía Cancelada[a], Hugo Destaillats[c], Marta I. Litter[a,b,d,*]

[a] Gerencia Química, Comisión Nacional de Energía Atómica, Av. Gral. Paz 1499, 1650 San Martín, Prov. de Buenos Aires, Argentina
[b] Consejo Nacional de Investigaciones Científicas y Técnicas, Av. Rivadavia 1917, 1033 Ciudad Autónoma de Buenos Aires, Argentina
[c] Indoor Environment Group, Energy Technologies Area, Lawrence Berkeley National Laboratory, Berkeley, CA, USA
[d] Instituto de Investigación e Ingeniería Ambiental, Universidad Nacional de General San Martín, Campus Miguelete, Av. 25 de Mayo y Francia, 1650 San Martín, Prov. de Buenos Aires, Argentina

ARTICLE INFO

Keywords:
Cr(VI)
Sonochemical reduction
Organic additives

ABSTRACT

The sonochemical (850 kHz) reduction of Cr(VI) (0.3 mM, pH 2, reactor open to air) was analyzed in the presence of different additives. The effects on Cr(VI) reduction efficiency of added formic acid (FA, 10 mM), citric acid (Cit, 2 mM), ethylenediaminetetraacetic acid (EDTA, 1 mM), methanol (MeOH, 0.1 M), ethanol (EtOH, 0.1 M), 2-propanol (2-PrOH, 0.1 M), *tert*-butanol (*t*-BuOH, 0.1 M), phenol (PhOH, 2 mM) and sodium lauryl sulfate (SLS, 1 mM) have been evaluated in comparison with the system in the absence of additives. Complete Cr (VI) reduction was obtained only when using EDTA (at 120 min) and Cit (at 180 min). Cr(III) complexes with these compounds or with their degradation products were detected as final products. For EDTA, Cit, *t*-BuOH, FA and SLS, the Cr(VI) decay could be adjusted to a zero-order kinetics; in the cases of MeOH, EtOH and 2-PrOH, there was a deviation from the zero-order kinetics. The Cr(VI) conversion increased in the order SLS (very low) < no additive ≅ MeOH ≅ EtOH ≅ 2-PrOH < FA < *t*-BuOH < PhOH < Cit < EDTA. The role of EDTA and Cit in stabilizing intermediate Cr(V) peroxo compounds and enhancing their direct transformation into different Cr(III) species is considered a major factor in the acceleration of Cr(VI) reduction processes. Mechanistic pathways are proposed.

1. Introduction

Hexavalent chromium (Cr(VI)) is a pollutant present in wastewaters of industrial processes such as leather tanning, paint manufacturing and electroplating. Due to its acute toxicity, carcinogenic and mutagenic effects and high mobility in water, its presence is of concern ([1] and references therein) and its maximum concentration in drinking water has been regulated to 50 $\mu g\, L^{-1}$ by the World Health Organization [2]. Cr(VI) treatment usually involves a reduction step to Cr(III), which is far less toxic than Cr(VI), and an essential trace metal in human nutrition [1]; Cr(III) can be easily removed from the solution as a solid waste after neutralization. Advanced Processes are promising technologies for Cr(VI) reduction; in particular, heterogeneous photocatalysis and nanozerovalent iron have been the most studied Advanced Processes for Cr(VI) reduction (see e.g. [1,3–5]). However, other Advanced Processes, such as sonochemical reduction, still merit research.

In general, most studies have focused on the sonochemical oxidation of organic pollutants, while the study of inorganic species is still scarce, especially through reductive processes (e.g. [6–10]). Cr(VI) reduction using ultrasound has been previously reported [11–14] with negligible reaction at low frequencies (20 kHz) [15]. Kathiravan and Muthukumar [14] proposed that Cr(VI) transformation by ultrasound is produced by reduction to Cr(III) by the direct action of H_2O_2 generated in the sonochemical process (see below); however, a complete mechanism was not provided by the authors. Ultrafine amorphous Cr_2O_3 powders have been produced by aqueous sonochemistry of ammonium dichromate, a process accelerated by the addition of ethanol [16]. This indicates that other alcohols and carboxylic acids can be added to promote Cr(VI) sonochemical reduction, in accordance with reports that indicate that organic compounds have a marked effect on ultrasonically induced chemical reactions [17]. Regarding the phase where Cr(VI) would react, according to Henglein and Kormann [18], it can hardly be expected that ionic species enter the gas phase and then it can be proposed that Cr(VI) reductive reactions take place at the interface or in the bulk solution. As said, H_2O_2 formation may occur, at least in part, in the liquid phase; therefore, reduction of Cr(VI) by H_2O_2 is highly feasible.

* Corresponding author at: Gerencia Química, Comisión Nacional de Energía Atómica, Av. Gral. Paz 1499, 1650 San Martín, Prov. de Buenos Aires, Argentina.
E-mail addresses: marta.litter@gmail.com, litter@cnea.gov.ar (M.I. Litter).

https://doi.org/10.1016/j.ultsonch.2018.05.014
Received 3 January 2018; Received in revised form 11 April 2018; Accepted 15 May 2018
Available online 18 May 2018
1350-4177/

Thus, in this paper, the presence of formic acid (FA), ethylenediaminetetraacetic acid (EDTA), citric acid (Cit), methanol (MeOH), ethanol (EtOH), 2-propanol (2-PrOH), *tert*-butanol (*t*-BuOH), phenol (PhOH) and sodium lauryl sulfate (SLS) has been evaluated regarding their effect on Cr(VI) reduction by ultrasound under air.

2. Experimental

2.1. Chemicals and materials

Potassium dichromate (99.9%), EtOH (> 99.9%), MeOH (99.7%) and PhOH (99%) were Merck, Cit (99%) and EDTA (99%) were Riedel de Häen, FA (99%) and SLS (> 92%) were Carlo Erba, 2-PrOH was Anedra (Research AG, 100%), and *t*-BuOH was Tedia (> 99.0%). Diphenylcarbazide was UCB for analysis, dissolved in acetone (Merck, 99.5%). Perchloric acid (70%, Biopack) was used for pH adjustment. All other reagents were of analytical grade and used as received. All solutions and suspensions were prepared with Milli-Q grade water (resistivity = 18 MΩ cm at 25 °C), Osmoion Apema.

2.2. Sonochemical reactor

2.2.1. Setup design

The sonochemical reactor was a 60 mm outer diameter, 2.5 mm thick and 50 mm height Pyrex tube, 350 mL total volume, jacketed with a 36 mm, 2 mm thick and 150 mm height outer diameter tube to allow water recirculation. An ultrasonic transducer type E/805/T(02) (Meinhardt-Ultraschalltechnik), with a DN 60 flange, emitting at 850 kHz, powered by an ultrasonic power generator type K 8-1 (Meinhardt-Ultraschalltechnik), was attached to the bottom of the reaction tube, in direct contact with the aqueous solution. An external jacket allowed water recirculation. The temperature of the cooling water was 25 °C; the temperature of the solution was 30 °C, reached 5 min after switching on the power and kept constant throughout the experiment. At the working frequency and conditions (850 kHz, ultrasonic intensity ≈ 10 W cm^{-2}), the maximum bubble radius and the collapse time can be estimated from Table 1 of reference [19] as 4.5 μm and 0.4 μs, respectively.

2.2.2. Calorimetry and dosimetry

In Appendix A, a complete description of the fundamentals and calculations performed to obtain the calorimetric and dosimetric parameters of the ultrasound system is provided, together with the corresponding references. The total power input by the transducer into the liquid (P_{ac}) was 51 W L^{-1} [20,21]. The $HO^{\cdot}$ generation rate obtained by the KI dosimetry [21] was 3.1 μM min^{-1}; this value, divided by the input power, gives a $HO^{\cdot}$ generation yield of 9.9×10^{-10} mol J^{-1}. With the Fricke dosimeter without and with Cu (II) [22], a Fe(III) generation rate of 5.9 μM min^{-1} was obtained, while in the experiment with Cu(II), the generation rate was 3.5 μM min^{-1}; the difference between these rates divided by 4 (0.6 μM min^{-1}) is the generation rate of $H^{\cdot}/HO_2^{\cdot}$ radicals [22]. H_2O_2 formation rate [20] was measured at 350 nm [23]; a constant H_2O_2 formation rate of 1.1 μM min^{-1} was obtained for sonolysis times shorter than 15 min. With this H_2O_2 generation rate and the $H^{\cdot}/HO_2^{\cdot}$ generation rate, the $HO^{\cdot}$ generation rate was calculated as 3.9 μM min^{-1}, close to 3.1 μM min^{-1}, the value obtained with KI.

2.2.3. Sonochemical experiments

The experiments were performed with 325 mL of a 0.3 mM Cr(VI) solution at pH 2 with the reactor open to air, adding the corresponding amount of organic additive in the particular experiments. All experiments were performed at least by duplicate and the standard deviation among replicates was never higher than 10%. The fitting of the experimental points was performed with Sigmaplot 12 software. Changes of pH at the end of all runs were negligible (ΔpH < 0.1). For all studied compounds, control experiments without ultrasound were performed under identical experimental conditions (30 °C, constant), as a measure of Cr(VI) thermal reduction, which was always found smaller than 5% even after 300 min; the solutions were always properly homogenized before sampling.

2.2.4. Analytical determinations

Samples (2 mL) were periodically taken from the reservoir and brought to 10 mL with distilled water. Cr(VI) was always determined by the diphenylcarbazide method at 540 nm [24] and, in some experiments, by the absorbance at 352 nm [25]; both techniques gave almost identical results, indicating that the Cr(V) concentration was always negligible [26].

Anions were analyzed by ionic chromatography (IC) using a Dionex ICS-5000 ion chromatograph with suppressed conductivity detection. An Anion Self-Regenerating Suppressor (ASRS 300-4 mm), and a carbonate suppressor (CRD 200-4 mm) were used, with an Ion Pack AS19-Analytical-4 × 250 mm column and an Ion Pack AG19 Guard-4 × 50 mm precolumn, and KOH at 1 mL min^{-1} isocratic flux as eluent, with the following linear concentration gradient: 10 mM KOH (0–6 min), 10–80 mM KOH (6–9 min), 80 mM KOH (9–21 min), 80–10 mM KOH (21.0–21.1 min), 10 mM KOH (21.1–24 min). For ammonium, a Cation Self-Regenerating Suppressor (CSRS 300–4 mm) was used, with an Ion Pack CS17-Analytical-4 × 250 mm column and an Ion Pack CG17 Guard-4 × 50 mm precolumn, and methanesulfonic acid (MSA) at 1 mL min^{-1} isocratic flux as eluent, with the following linear concentration gradient: 2 mM MSA (0–11 min), 2–7 mM MSA (11–11.1 min), 7 mM MSA (11.1–22 min), 7–2 mM MSA (22–22.1 min), 2 mM MSA (22.1–24 min). The temperature of columns and detectors were 30 and 35 °C, respectively, and the injection loop was 100 μL.

PhOH was determined by HPLC using a Cecil Adept CE4900 HPLC chromatograph, in the following conditions: reversed phase C-18 column (Grace-Alltech GraceSmart RP 18, 250 × 4.6 mm; 5 μm particle size), water:MeOH solution (70:30) as eluent, 1 mL min^{-1} flow rate, 200 μL loop, detection at 280 nm.

TOC (total organic carbon) was measured with a Shimadzu 5000-A TOC analyzer in the TOC mode.

For dissolved oxygen measurement, a Hach SensIon 156 dissolved oxygen meter was used (detection limit 0.1 mg O_2 L^{-1}).

UV–Vis absorption measurements were performed employing a PG Instruments UV–visible spectrophotometer, model T80+. UV–Vis absorption spectra were performed in a Hewlett-Packard diode array UV–visible spectrophotometer, model HP 8453 A.

3. Results

In Fig. 1, results of Cr(VI) (0.3 mM) ultrasonic decay in the presence of different additives at pH 2 with the reactor open to air are shown. The pH was that of previous works of the group on Cr(VI) photocatalytic reduction over TiO_2 [26–29]. At this concentration and pH, the main Cr(VI) species is $HCrO_4^-$ [30]. The concentration of Cit was 2 mM, the optimum found for TiO_2 Cr(VI) photocatalytic system [26], while the concentration of the other carboxylic acids, SLS and PhOH were selected to correspond approximately to the same initial TOC of 2 mM Cit. The concentration of the alcohols (0.1 M) was similar to that used in the Cr(VI) photocatalytic reduction in the presence of MeOH published before [31]; under these conditions, the thermal reduction of Cr(VI) by MeOH can be neglected. Fig. 1(a) is the plot for the Cr(VI) decay in the absence of additives and in the presence of carboxylic acids, *t*-BuOH, PhOH and SLS, while Fig. 1(b) is the plot in the presence of MeOH, EtOH and 2-PrOH.

A linear Cr(VI) decay is observed for the conditions of Fig. 1(a) while a deviation of this kinetic behavior is observed for the results of Fig. 1(b). For comparison, zero order rate constants (k_0) taken from the points of Fig. 1(a) and initial zero order rate constants ($k_{0,i}$) (up to 15 min) taken from the points of Fig. S1(b) are presented in Table 1.

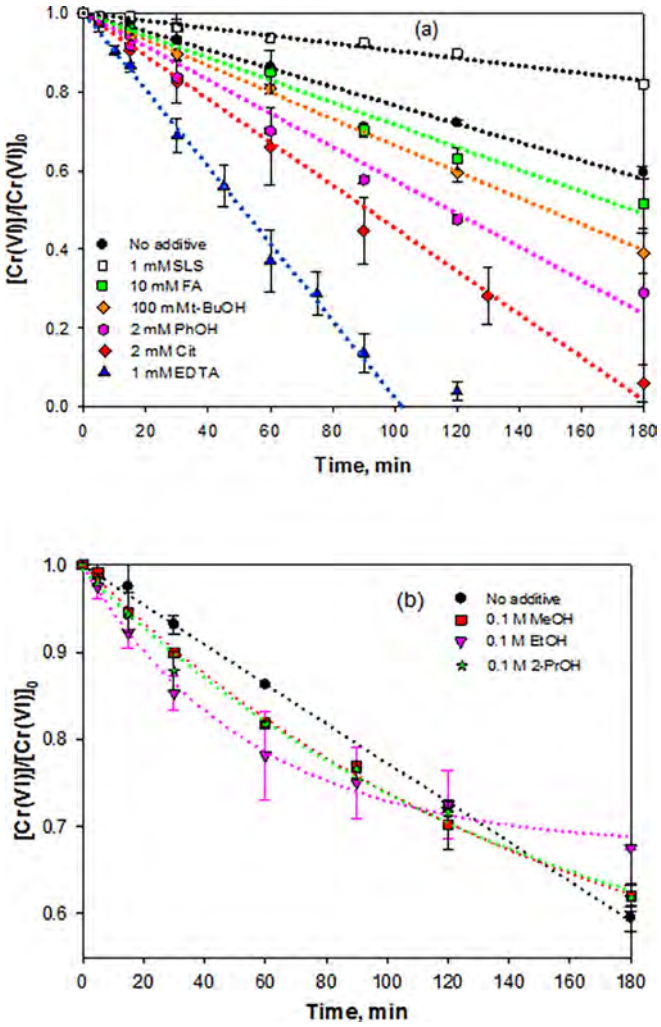

Fig. 1. Temporal profile of normalized Cr(VI) concentration ([Cr(VI)]/([Cr(VI)]$_0$) during the sonochemical experiments of Cr(VI) in the presence of different additives: (a) with EDTA, Cit, FA, SLS, PhOH and *t*-BuOH; (b) with MeOH, EtOH and 2-PrOH. Conditions: [Cr(VI)]$_0$ = 0.30 mM, pH 2 ($HClO_4$), T = 30 °C, reactor open to air. Dotted lines are only for a better visualization of points and do not correspond to any fitting model.

The Table also shows the percentage of Cr(VI) decay at 180 min, and the vapor pressure of volatile compounds calculated from the Henry constant [32] in water at the used concentration. As the vapor pressures are those of the pure compounds, this explains the higher vapor pressure of *t*-BuOH compared with MeOH under our experimental conditions, despite pure MeOH is more volatile than pure *t*-BuOH at a given temperature. For the systems without additives and with nonvolatile compounds (i.e., EDTA, Cit, PhOH and SLS), the vapor pressure is that of water at 25 °C.

Dissolved O_2 evolution during the experiments presented no significant differences among the different conditions, and the averaged results are shown in Fig. S2. A final value of O_2 concentration = 0.5 mg L^{-1} was measured at t = 180 min, indicating that anoxic conditions were never reached during the experiments.

A separate sonolytic experiment of water at pH 2 (with $HClO_4$, no Cr (VI) or additives), open to air, revealed that 92 μM H_2O_2 were formed after 180 min of insonation (Fig. S3). The evolution of the H_2O_2 concentration followed a zero order rate law, according to Eq. (1):

$$[H_2O_2] = k_{H_2O_2} \times t \quad (1)$$

where $k_{H_2O_2}$ is the kinetic constant. As indicated in Section 2.2.2, a value of 1.1 μM min^{-1} was obtained.

The mineralization of all organic compounds measured by TOC was negligible (< 2%, standard error around 5%). Cr(III) formation was proved in the case of the experiments with EDTA and Cit, as shown by the bands in the range 540–580 nm in the spectra of the final solution, i.e., when almost complete Cr(VI) reduction was reached (Fig. 2). The concentration of Cr(III)-EDTA was estimated as 0.16 mM using ε_{540} = 140 M^{-1} cm^{-1} [29] while that of Cr(III)-Cit was 0.14 mM using ε_{575} = 45 M^{-1} cm^{-1} [33]; in both cases, around half of the reduced Cr (VI) ended in complexed Cr(III). The spectrum of the experiment without additives (not included) was almost identical to that with FA, and no Cr(III) could be detected after 180 min of reaction in both experiments, but this could be ascribed to the small ε_{575} of Cr(III) when not complexed (13 M^{-1} cm^{-1}) [34].

The change in the spectrum of the Cr(VI) solution in the presence of Cit during a sonochemical experiment is included in Appendix A (Section S6, Fig. S4). Fig. S4 clearly indicates the decrease of the Cr(VI) band at 360 nm of chromate in solution (e.g., [35]).

For the EDTA and Cit systems, the degradation products were analyzed by IC at final times under different conditions. FA, acetic acid (AA), nitrate and nitrite (from EDTA) were the only products detected. Table 2 indicates the concentrations.

In the case of PhOH, the HPLC analysis indicated a final PhOH

Table 1
Zero order rate constants (k_0) for the Cr(VI) decay extracted from Fig. 1(a), initial zero order rate constants ($k_{0,i}$) (up to 15 min) from Fig. S1(b) and percentage of Cr (VI) decay at 180 min taken from both Fig. 1(a) and (b). P_V is the vapor pressure at 25 °C of the compounds calculated from the Henry constants in water [32] at the used concentration and of water for the reaction without additives, and with EDTA, Cit, PhOH and SLS. H^{cp} is the Henry constant of the compounds in water at 25 °C [32].

Sample	k_0 (M min^{-1}) × 10^7	% Cr(VI) decay at 180 min	P_V (kPa) [30,32]	H^{cp} (mol L^{-1} kPa^{-1}) [32]
No additive[a]	6.9	40	3.2	–
SLS (1 mM)	1.8	18	3.2	–
MeOH (0.1 M)	10.5[c]	38	5.0×10^{-2}[b]	2.0
EtOH (0.1 M)	15.3[c]	32	5.3×10^{-2}[b]	1.9
2-PrOH (0.1 M)	11.4[c]	38	7.7×10^{-2}[b]	1.3
FA (10 mM)	8.4	48	1.1×10^{-4}[b]	88
t-BuOH (0.1 M)	10.1	61	1.4×10^{-1}[b]	0.69
PhOH (2 mM)	15.3	71	3.2	28
Cit (2 mM)	16.5	94	3.2	3×10^{16}
EDTA (1 mM)	27	100[d]	3.2	–

[a] H_2O with perchlorate at pH 2.
[b] Calculated from the Henry constant [32].
[c] Initial zero order rate constants ($k_{0,i}$) (up to 15 min).
[d] Estimated (96% at 120 min).

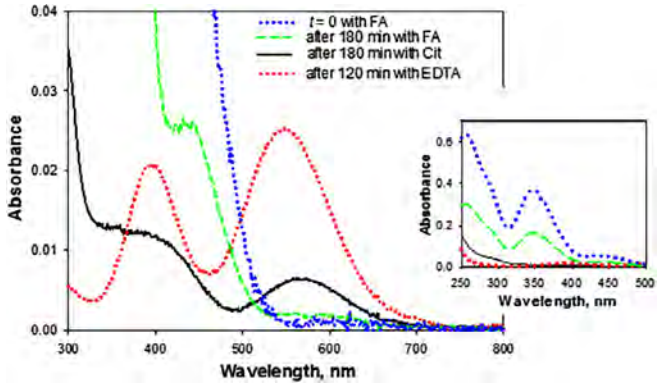

Fig. 2. UV–Vis spectra of the solutions obtained at the beginning of the run with FA and at end of the runs of Fig. 1(a) for EDTA, Cit and FA. Inset: spectra in the 250–500 nm range.

Table 2
Quantification of products found at the end of the sonochemical transformation of Cr(VI) in the presence of EDTA and Cit with the reactor open to air, and with Cit under Ar and air bubbling. Conditions: $[Cr(VI)]_0$ = 0.30 mM, [Cit] = 2 mM or [EDTA] = 1 mM, pH 2 ($HClO_4$), T = 30 °C, bubbling flow rate = 0 (no bubbling, reactor open to air) or 0.5 L min^{-1} (Ar or air bubbling).

Additive/reaction time	[FA] (μM)	[AA] (μM)	$[NO_3^-]$ (μM)	$[NO_2^-]$ (μM)
EDTA/120 min open to air	167	113	85	2
Cit/180 min open to air	35	22	94	ND
Cit/180 min/Ar bubbling	31	15	ND	ND
Cit/180 min/air bubbling	37	28	40	ND

ND: not detected.

concentration of 1.75 mM (82.5% degradation), without detection of catechol or hydroquinone; small amounts of benzoquinone (not quantified) and another unidentified aromatic product were identified.

Neither perchlorate ($[ClO_4^-] \approx 10$ mM) transformation nor the presence of its possible reduction byproducts (i.e., chlorate, chlorite, hypochlorite and chloride) was detected.

The effect of the working atmosphere and of the concentration of dissolved O_2 on the Cr(VI) decay in the presence of Cit was studied using either Ar ($[O_2] < 0.1$ mg L^{-1}) and air ($[O_2] = 8.2$ mg L^{-1}, constant) bubbling (flow rate = 0.5 L min^{-1}). The results are shown in Fig. 3.

As can be observed, the reduction of Cr(VI) under Ar bubbling follows a zero-order rate that is almost identical to the one obtained with the reaction open to air (15.6×10^{-7} M min^{-1} vs. 16.5×10^{-7} M min^{-1}, respectively). Under air bubbling, Cr(VI) evolution up to 180 min also follows a zero-order rate, but the calculated rate (9×10^{-7} M min^{-1}) is almost half the rate obtained without bubbling; interestingly, between 180 min and 270 min, the air bubbling was stopped, the reactor was left open to air, and an increase of the rate was observed (12.6×10^{-7} M min^{-1}), indicating that the bubbling affected the generation of reactive species. Indeed, the $HO^{\cdot}$ generation yields obtained by KI dosimetry under air and Ar bubbling were 7.4 and 4.9×10^{-10} mol J^{-1}, respectively, i.e., lower values than that obtained without bubbling (9.9×10^{-10} mol J^{-1}). These results are unexpected, as an increase in the $HO^{\cdot}$ generation yield is always reported both at the higher $[O_2]$ under air bubbling, and when using Ar bubbling. As expected, nitrate was not detected in the experiment performed under Ar bubbling, and a decrease in the concentration of nitrate formed after 180 min was observed in the experiment under air bubbling (Table 2).

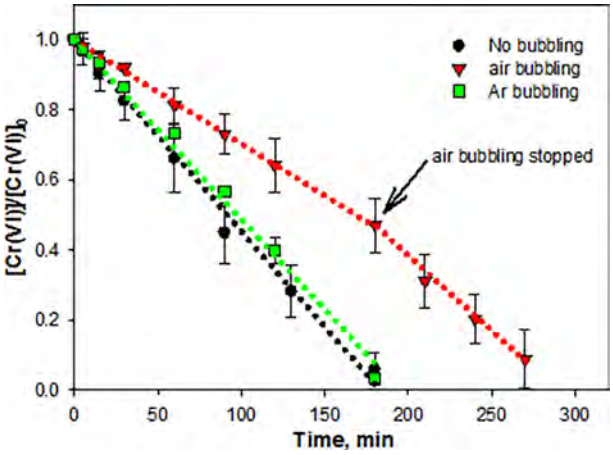

Fig. 3. Temporal profile of normalized Cr(VI) concentration ([Cr(VI)]/([Cr(VI)]$_0$) during the sonochemical experiments of Cr(VI) in the presence of Cit under different atmospheres: open to air (no bubbling), Ar ($[O_2] < 0.1$ mg L^{-1}) or air ($[O_2] = 8.2$ mg L^{-1}, constant) bubbling. Conditions: $[Cr(VI)]_0$ = 0.30 mM, [Cit] = 2 mM, pH 2 ($HClO_4$), T = 30 °C, bubbling flow rate = 0 (no bubbling) or 0.5 L min^{-1} for the reactor open to air. Dotted lines are only for a better visualization of points and do not correspond to any fitting model.

4. Discussion

Ultrasound irradiation (15 kHz–1 MHz) in water produces acoustic cavitation microbubbles of gas that nucleate, grow and implode in extremely small intervals of time (100 ns), the gas reaching very high local temperatures and pressures (4.000–10.000 K and 1.000–10.000 bars), and releasing localized large quantities of energy in "hot spots" within the liquid. In Appendix A, the most relevant reactions taking place in these processes are presented, together with some of the corresponding references. During a cavitation event, three different sites exist for chemical reaction [17,36]. First, the interior of the collapsing gas bubbles, where pyrolysis reactions in the gas phase take place with the production of hydroxyl radicals ($HO^{\cdot}$) and hydrogen atoms ($H^{\cdot}$) from water (Eq. (S1)). Volatile compounds will be incorporated in this phase and undergo thermolysis, yielding radicals which recombine, react with other gaseous species in the cavity, or diffuse out of the bubble into the bulk fluid medium, where they react with dissolved molecules. Molecular hydrogen and H_2O_2 are produced (Eqs. (S2) and (S3)). Thermal gas-phase reactions of volatile substances also take place. In the presence of oxygen or air, atomic oxygen ($O^{\cdot}$) is produced by a sonolytic primary process (Eq. (S4)), leading to additional $HO^{\cdot}$ (Eq. (S5)). Other pathways can contribute to H_2O_2 formation (e.g., Eqs. (S7)–(S10)). The second region is the interfacial region between the gas bubbles and the bulk solution, with relatively lower temperatures but still high enough to induce radical thermal reactions from accumulated nonvolatile hydrophobic solutes and surfactants. The interface is characterized by elevated temperatures and high $HO^{\cdot}$ concentration (around 10^{-2} M [22]). Therefore, H_2O_2 can be produced either in the gas phase or in the interface, migrating out to the bulk solution [18,37]. Reaction (S11), attributed to the reaction of hot $H^{\cdot}$ with gaseous water, increases the amount of $HO^{\cdot}$. Sonochemistry in the presence of O_2 is frequency dependent: molecular oxygen splitting is favored at high frequency ultrasound while scavenging of $H^{\cdot}$ with O_2 occurs at low frequency [38]. However, in any case, in the presence of O_2, $H^{\cdot}$ is rapidly converted into hydroperoxyl radicals ($HO_2^{\cdot}$, Eq. (S6)), making negligible H_2 production. The third region is the bulk solution, to where the radicals produced in the bubbles and in the interface (mainly $HO^{\cdot}$ and $H^{\cdot}$) escape and undergo scavenging reactions with other solutes [37,39]. Secondary reactions leading to H_2O_2 formation can take place in the liquid phase [40]. Water soluble substances will

remain in this aqueous phase, and oxidative degradation will proceed via species produced in the other two regions, such as $HO^{\cdot}$ and H_2O_2 that migrate out into the bulk solution. Recent works have proved that nonequilibrium plasma conditions exists in the collapsing bubbles, with the formation of other reactive species such as O_2^{+} and excited $HO^{\cdot}$ [19,41,42].

In air (N_2 + O_2), N_2 can react with O, giving NO and $N^{\cdot}$ (Eq. S13) and $N^{\cdot}$ can also be formed by a sonolytic primary process (Eq. (S14)). However, Eq. (S14) would be a minor reaction compared with Eq. (S4), taking into account the lower bond energy of the O_2 double bond compared with that of the N_2 triple bond [43]. Reactions described by Eqs. (S13)–(S18) will lead to HNO_3, HNO_2 and other nitrogenated compounds.

Eqs. (S1)–(S18) describe the reactions taking place in sonochemical aqueous systems in the absence of other chemical species. When organic additives are present in the system, secondary radicals can be formed by direct thermal decomposition in the interfacial region or in the cavities (Eq. (2)), and other secondary radicals ($R^{\cdot}$) can be formed by reaction with $HO^{\cdot}$ or $H^{\cdot}$ (in deoxygenated media) (Eq. (3)) [9,18,39,44–46]. Some of these radicals are reductants able to accelerate reductive processes.

$$RH + H_2O \rightarrow \text{pyrolysis radicals} \quad (2)$$

$$RH + HO^{\cdot}\ (H^{\cdot}) \rightarrow R^{\cdot} + H_2O\ (H_2) \quad (3)$$

Thus, Cr(VI) reduction could take place through the following steps: 1) reduction by $H^{\cdot}$ or H_2, 2) reduction by H_2O_2 generated in Eqs. (S3) and (S7)–(S10), 3) reduction by pyrolysis radicals formed by Eq. (2), 4) reduction by $R^{\cdot}$ formed through Eq. (3). Except when Ar was bubbled, oxygen was present in all experiments during the whole run (Fig. S2); therefore, all processes involving $H^{\cdot}$ will be negligible. The formation of the highly reducing hydrated electrons can be discarded in sonochemical systems at acid pH [17,44]. It is important to remark that the thermal reduction of Cr(VI) either in the absence or in the presence of the additives (control experiments) is negligible, indicating that Cr(VI) can be reduced only under ultrasound irradiation.

The homogeneous chemistry between Cr(VI) and H_2O_2 in water is complex and involves different reactions (ligand exchange, proton transfer, oligomerization, and redox processes) [47]. The global reaction in acid/neutral media can be formulated as follows:

$$2\ HCrO_4^{-} + 3\ H_2O_2 + 8\ H^{+} \rightarrow 2Cr^{3+} + 8\ H_2O + 3\ O_2 \quad (4)$$

In Appendix A, the mechanistic pathways leading to Cr(III) formation by H_2O_2 are indicated, together with the corresponding references (Eqs. (S26)–(S33)). Briefly, at pH < 4 [48], this reaction involves the formation of a monoperoxochromium(VI) complex (Eq. (S26)), the rate limiting step, followed by reactions with H_2O_2 with formation of Cr(V) peroxo- and oxocomplexes ending in the transformation of the tetraperoxocomplex $[Cr^{V}(O_2)_4]^{3-}$ to Cr(III) (Eq. (S33)). The concentration of these Cr(VI) and Cr(V) compounds in the present work was always very low, as the band at $\lambda > 500$ nm of diperoxo Cr(VI) and peroxo Cr (V) compounds under acidic conditions [47,49] was never detected (see Fig. 2). Reactions of Cr(V) chemical species like $[Cr^{V}(O_2)_4]^{3-}$ with H_2O_2 have also the ability of generating $HO^{\cdot}$ in a Fenton type reaction ([49,50] and references therein), giving a cyclic generation of Cr(VI)/Cr (V) and additional $HO^{\cdot}$:

$$Cr(V) + H_2O_2 \rightarrow Cr(VI) + HO^{\cdot} + OH^{-} \quad (5)$$

According to Eq. (4), the Cr(VI) reduction rate in the absence of additives must be 2/3 the H_2O_2 generation rate in the absence of Cr(VI) (1.1 μM min^{-1}, Section 2.2.2), i.e., 0.75 μM min^{-1}, in close agreement with the Cr(VI) reduction rate of 0.69 μM min^{-1}, determined from Table 1 and $[Cr(VI)]_0$ = 0.3 mM; the difference can be ascribed to Cr (VI)-mediated peroxide disproportionation [47]. It has been reported [51] that a high H_2O_2 excess ($[H_2O_2] > 10 \times [Cr(VI)]$) is required to achieve complete Cr(VI) thermal reduction under similar pH and Cr(VI) concentration as those used here; thus, the present system seems to use more efficiently H_2O_2 as Cr(VI) reductant. As the Cr(VI) reduction rate is constant throughout the experiment, it was concluded that the decrease in O_2 concentration revealed by Fig. S2 does not influence the generation rate of H_2O_2.

When organic compounds are added to the sonolytic system, they may react through Eqs. (2) and (3), originating radicals able to transform Cr(VI) into Cr(V), Cr(IV) and the final stable Cr(III) product plus oxidation products (R_{ox}).

$$Cr(VI)/(V)/(IV) + R^{\cdot} \rightarrow Cr(V)/(IV)/(III) + R_{ox} \quad (6)$$

In fact, the generation of secondary reducing radicals was used to explain the accelerating effect of ethanol in the sonochemical synthesis of Cr_2O_3 from ammonium dichromate [16]. A similar process was proposed for the sonochemical formation of gold particles from Au(III) reduction [7,46] and in the sonolytic reduction of MnO_2 [52–54].

As said before, it is highly probable that reduction of Cr(VI) ions takes place at the interface or in solution; the carboxylic acids and PhOH will react in solution, while the alcohols will be enriched in the bubble vapor, and will react in the gas phase. SLS can be expected to concentrate in the interface, with the alkyl moiety in the gas phase. Therefore, it can be proposed that the experiments with the organic compounds will obey to different kinetic behaviors, depending on the phase where the reaction of the additive takes place. A similar explanation was given to explain the different reactivity of volatile, low-volatility compounds and charged non-volatile water soluble species [55,56].

First, non-volatile water soluble substances like EDTA and Cit, which do not partition to the vapor phase or to the interface, will remain in the aqueous phase. Degradation of these compounds will proceed via oxidative species produced at the cavitation bubble, such as $HO^{\cdot}$, which will migrate out into bulk solution [18,37], generating reducing radicals [55]. The presence of these carboxylic acids such as EDTA and Cit, as in photocatalytic systems [26–29], improves the rate and efficiency of the Cr(VI) removal, as it can be seen in Fig. 1(a). Moreover, their presence would inhibit the detrimental Cr(V)/(IV)/(III) reoxidation by oxidative species like $HO^{\cdot}$, which will attack preferentially these species (present at high concentrations). In fact, it has been found that Cr(III)-EDTA complexes oxidize very slowly under ultrasound to Cr(VI) [56]. This includes the scavenging of $HO^{\cdot}$ formed during the transformation of Cr(V) by Eq. (5). Although an inhibiting scavenging of reducing radicals $R^{\cdot}$ will take place when O_2 is present (Eq. (7)), the intermediate peroxy species can still be expected to be able to reduce Cr(VI) [72].

$$R^{\cdot} + O_2 \rightarrow ROO^{\cdot} \quad (7)$$

The higher rate of reaction of EDTA with $HO^{\cdot}$ compared with that of Cit ($k_{HO^{\cdot}}$ = 4.0 × 10^8 vs. 5.0 × 10^7 M^{-1} s^{-1} [57])[1] would explain the higher Cr(VI) decay in the case of the former. Additionally, Cit and EDTA and their degradation products greatly stabilize Cr(V) species (e.g., the monoperoxochromate(V)) by complexation, as already proven by the group in previous works [26,27], and enhance its decomposition to Cr(III) [58,59]. Although no mineralization of the compounds is observed from TOC results, similarly to that observed by Frim et al. [55] (who attributed the lack of EDTA mineralization to the presence of Cr(III)), the detection of FA and AA in the experiments with Cit and EDTA (Table 2) indicates that these compounds are degraded to intermediates, most probably by $HO^{\cdot}$ attack. As said before, in air, HNO_2, HNO_3 and other nitrogenated products can be formed (Eqs. (S13)–(S18)). As indicated above, in the experiments with Cit and EDTA, nitrate is formed at a concentration lower than 100 μM, while

[1] Although $HO^{\cdot}$ may be formed in a different phase than the scavenger, the rate constants of reaction with $HO^{\cdot}$ to be considered here will be, as an approximation, those known from homogeneous processes (e.g., radiation chemical studies).

traces of nitrite (2 μM) were also detected in the experiment with EDTA. In this last case, nitrogen species can arise not only from N_2 but also from EDTA degradation.

The sonochemical PhOH degradation is proposed to take place also in the aqueous phase by $HO^{\cdot}$, because PhOH is a hydrophilic substance with low vapor pressure (Table 1), not diffusing to a significant extent into the cavitation bubble and, consequently, presenting negligible pyrolytic degradation (e.g., [60]). It has been established that the degradation occurs mainly in the bulk solution [61]. In our experiments, no PhOH mineralization was measured even after 180 min of reaction, and benzoquinone and other non-identified aromatic compound were the only compounds detected after analysis. PhOH was the most efficient non-complexing additive studied, and this can be related with the primary by-products formed, catechol and hydroquinone (not detected in our experiments), which can directly reduce Cr(VI) by a fast thermal reaction at low pH [62,63].

On the other hand, as said before, volatile substances that enter into the cavitation bubble will mainly undergo thermolysis. As it can be seen in Fig. 1(b), alcohols do not accelerate very much Cr(VI) reduction in comparison with the system in the absence of additives, and a deviation from the zero order kinetic regime followed by the carboxylic acids and PhOH takes place at around 15 min (except for *t*-BuOH). This can be explained by volatilization of the alcohols in the gas phase; this volatilization cannot be noticed from TOC evaluation, as the alcohols are degraded to organic intermediates (e.g., formaldehyde or FA in the case of MeOH). To explain the different reactivities of alcohols, it is possible to follow the aspects suggested some years ago concerning the hydrophobicity order, MeOH < EtOH < 2-PrOH < *t*-BuOH [18,39,64], and the surface excess at the vapor-liquid interface [45,52], that parallel roughly the order indicated in Table 1 for the initial rates, vapor pressure and percentage of Cr(VI) conversion at 180 min. The more hydrophobic the alcohol, the more it will accumulate at the gas/water interface [45]. Thus, we prefer to associate the rates with the vapor pressures, listed in Table 1 (water being the main component of the gas phase). Although the values of the vapor pressure in this Table are given at 25 °C, it is possible to assume the same trend at higher temperatures due to similar vaporization enthalpies (around 35–40 kJ mol^{-1}) [30]. It must be pointed out also that, at higher vapor pressures, the cavitation process is less energetic, dampening the cavitation impact [17], forming thus less reactive species. Reaction of $HO^{\cdot}$ with the alcohols at cavitation sites competes with Eq. (S3), reducing H_2O_2 production [40,65]; this can decrease the rate of Cr(VI) decay. It can be proposed that the Cr(VI) reduction observed in these cases proceeds more probably by the very well-known strong reducing α-hydroxyalkyl radicals produced by $HO^{\cdot}$ attack to the alcohols, having redox potentials [66] enough to reduce Cr(VI) up to Cr(III). According to Okitsu et al. [54], at high concentration of the alcohols, Cr(VI) reduction is more probably produced by reducing radicals.

Interestingly, the reaction of *t*-BuOH with $HO^{\cdot}$ does not produce a reducing radical; however, it is the most efficient of the alcohols here studied, giving a linear kinetics and being included in Fig. 1(a). It has been reported that although the sonolytic *t*-BuOH degradation takes place mainly by pyrolysis in the cavitation bubble due to its high vapor pressure (Table 1), it produces CO [65,67], which would diffuse into the liquid phase where it can reduce Cr(VI) while being transformed into CO_2, as reported in a different system [68]. Pyrolysis would be a minor mechanism in the case of the other alcohols because of their lower vapor pressure (Table 1). It has to be added that, according to Sostaric et al. [52], at least in the case of MnO_2 reduction, the efficacy can be directly related to the Gibbs surface excess concentration of the alcohol at the air/water interface, irrespective of the bulk solution concentration or type of alcohol.

As the vapor pressure of FA is lower than those of the alcohols (Table 1), the contribution of pyrolysis could be neglected [18], and the suggested deviation of the linear kinetics by vaporization would be rather small; this allows its inclusion in Fig. 1(a), with a linear Cr(VI) decay. However, FA is indicated as a very inefficient scavenger in sonochemical reactions, because it is not readily accumulated in the interfacial region, having a low hydrophobicity [18,69]. FA does not inhibit (or to a low extent) H_2O_2 formation at the concentrations used here and its decomposition in sonolytic systems into radicals plays a minor role, the main reactions being thermal dehydration and decarboxylation. However, and in contrast to the system in the absence of additives, FA would still scavenge $HO^{\cdot}$ avoiding Cr(V)/(IV)/(III) reoxidation and generating at the same time the strong reducing carboxyl radical ($^{\cdot}CO_2^-$, $E^0 = -1.9$ V) [70], which enhances Cr(VI) reduction:

$$HCOOH + HO^{\cdot} \rightarrow {}^{\cdot}CO_2^- + H_2O + H^+ \quad (8)$$

Additionally, no complexes of FA with Cr(V) and Cr(IV) have been reported, in contrast to EDTA or Cit, and the favorable stabilization of Cr(V) is not possible with this organic acid.

Non-volatile hydrophobic compounds and surfactants, while not passing into the vapor phase, partition to the interface. As observed for other surfactants, SLS can be expected to concentrate in the interface, with the alkyl moiety in the gas phase and, thus, exposed to both pyrolysis and reaction with $HO^{\cdot}$ [71]. The alkyl radical formed after $HO^{\cdot}$ attack to SLS would probably be a secondary carbon radical (–C$^{\cdot}$H–), with minor amounts of primary carbon and methyl radicals [72], all of them non-reducing radicals that would decay by other mechanisms [72]. On the other hand, SLS would greatly inhibit H_2O_2 formation by Eq. (S3), as $HO^{\cdot}$ would be efficiently captured by the high concentration of this compound in the same place where their recombination takes place [36]. These effects would cause a net decrease on Cr(VI) reduction rate, as is clearly appreciated in Fig. 1(a). Although H_2O_2 can still be formed according to Eqs. (S7)–(S10), and considering reactions (S7) and (S8) to be the most relevant, the rate of H_2O_2 formation can be calculated as 0.3 μmol L^{-1} min^{-1}, i.e., half the rate of $H^{\cdot}/HO_2^{\cdot}$ formation (0.6 μmol L^{-1} min^{-1}, see Appendix A). This H_2O_2 generation rate is equivalent to a Cr(VI) reduction rate of 0.2 μmol L^{-1} min^{-1} according to Eq. (4), almost identical to the Cr(VI) reduction rate with SLS (0.18 μM min^{-1}, determined from Table 1 and $[Cr(VI)]_0 = 0.3$ mM). A analogous inhibitory effect by a structurally similar surfactant (sodium dodecyl sulfate) has been reported in the degradation of an organic contaminant [73].

From the analysis of the results included in Fig. 3, it can be concluded that the bubbling system used causes a decrease in the reactor performance; indeed, once the air flow was stopped, an increase in the Cr(VI) reduction rate was observed. This is in contrast to the results obtained by Pflieger et al. [38] and references therein, where the stirring and the gas flow increase the reactor performance due to a more homogeneous distribution of the bubbles in the reactive volume (although a four times lower ratio of gas flow over treated volume was used). The decrease in the $HO^{\cdot}$ generation yield under air confirms this lower efficiency due to the bubbling, as in the literature an increase in the $HO^{\cdot}$ and/or H_2O_2 generation yield is usually observed when increasing $[O_2]$ [21,37,43], except when noble gases are used; however, even under those conditions, the combination O_2/Ar increases H_2O_2 generation yield [38,74]. Under Ar, the Cr(VI) reduction rate is almost equal to that obtained with the reactor open to air; however, as the $HO^{\cdot}$ generation yield is decreased 50% under Ar, it is clear that other species such as $H^{\cdot}$ and/or H_2 [7,61,74] are contributing to Cr(VI) reduction. Finally, Table 2 indicates that a decrease in the concentration of nitrate produced is also observed under air bubbling; this reinforces the assumption that the main effect of the bubbling is a decrease in the generation rate of reactive species and not the generation of other species that might compete with Cr(VI) for the generated H_2O_2 (e.g. nitrite, by its oxidation to nitrate by H_2O_2 [75]).

An additional remark is that perchlorate ($[ClO_4^-] \approx 10$ mM) could compete with Cr(VI) for the reducing radicals generated during the reaction; however, as said, no perchlorate transformation or the presence of its possible reduction byproducts was detected, indicating that

perchlorate is inert in the studied system, as observed in a previous work [76].

5. Conclusions

Sonolysis is a viable technology for Cr(VI) treatment, especially in the presence of EDTA and Cit, compounds usually found together with Cr(VI) in several effluents. Reactions with the reactor open to air indicate that no especial precautions to avoid oxygen in the system have to be taken.

The Cr(VI) conversion increased in the order SLS < no additive ≅ MeOH ≅ EtOH ≅ 2-PrOH < FA < *t*-BuOH < PhOH < Cit < EDTA. The Cr(VI) decay was dependent on the chemical nature of the additive, the place where these compounds react with reactive species ($HO^{\cdot}$) or decompose by pyrolysis being relevant to explain the different efficiencies. A mechanism involving the action of H_2O_2 generated by several steps and the reducing radicals of the additive, leading to Cr(V), Cr(IV) and Cr(III), are proposed. The role of EDTA and Cit in stabilizing intermediate Cr(V) peroxo compounds and enhancing their direct transformation into different Cr(III) species was discussed, and is considered to be a major factor in the acceleration of Cr(VI) conversion processes.

Although Cit and EDTA seem to be the most promising additives, their Cr(III) complexes should be removed before the discharge of the treated effluent, as trace amounts of H_2O_2 can reoxidize these complexes to Cr(VI) under neutral conditions, although at lower rates than inorganic Cr(III) [56,77]. Comparing both compounds, Cit would be more convenient than EDTA as its Cr(III) complex is oxidized to Cr(VI) by H_2O_2 300 times slower than Cr(III)-EDTA [77]. Additionally, Cit is an environmentally friendly compound [56].

Acknowledgments

This work was performed as part of Agencia Nacional de Promoción Científica y Tecnológica PICT2011-0463, 2015-208 and PICT 3640 projects.

Appendix A. Supplementary data

Supplementary data associated with this article can be found, in the online version, at http://dx.doi.org/10.1016/j.ultsonch.2018.05.014.

References

[1] M.I. Litter, Last advances on TiO_2-photocatalytic removal of chromium, uranium and arsenic, Curr. Opin. Green Sustainable Chem. 6 (2017) 150–158.
[2] Guidelines for Drinking-water Quality, fourth ed., World Health Organization, Geneva, 2011.
[3] M.I. Litter, Mechanisms of removal of heavy metals and arsenic from water by TiO_2-heterogeneous photocatalysis, Pure Appl. Chem. 87 (2015) 557–567.
[4] R. Mukherjee, R. Kumar, A. Sinha, Y. Lama, A.K. Saha, A review on synthesis, characterization and applications of nano-zero valent iron (nZVI) for environmental remediation, Crit. Rev. Environ. Sci. Technol. 46 (2016) 443–466.
[5] V.N. Montesinos, N. Quici, E.B. Halac, A.G. Leyva, G. Custo, S. Bengio, G. Zampieri, M.I. Litter, Highly efficient removal of Cr(VI) from water with nanoparticulated zerovalent iron: understanding the Fe(III)–Cr(III) passive outer layer structure, Chem. Eng. J. 244 (2014) 569–575.
[6] Pankaj, Aqueous inorganic sonochemistry, in: Pankaj, M. Ashokkumar (Eds.), Theoretical and Experimental Sonochemistry Involving Inorganic Systems, Springer Science & Business Media, Dordrecht, Heidelberg, London, New York, 2010, pp. 213–272.
[7] Y. Nagata, Y. Mizukoshi, K. Okitsu, Y. Maeda, Sonochemical formation of gold particles in aqueous solution, Radiat. Res. 146 (1996) 333–338.
[8] J.L. Capelo, I. Lavilla, C. Bendicho, Room temperature sonolysis-based advanced oxidation process for degradation of organomercurials: application to determination of inorganic and total mercury in waters by flow injection-cold vapor atomic absorption spectrometry, Anal. Chem. 72 (2000) 4979–4984.
[9] Y. Mizukoshi, E. Takagi, H. Okuno, R. Oshima, Y. Maeda, Y. Nagata, Preparation of platinum nanoparticles by sonochemical reduction of the Pt(IV) ions: role of surfactants, Ultrason. Sonochem. 8 (2001) 1–6.
[10] B. Neppolian, A. Doronila, F. Grieser, M. Ashokkumar, Simple and efficient sonochemical method for the oxidation of arsenic(III) to arsenic(V), Environ. Sci. Technol. 43 (2009) 6793–6796.
[11] Pankaj, M. Chauhan, Sonochemical study on multivalent cations (Fe, Cr, and Mn), in: Pankaj, M. Ashokkumar (Eds.), Theoretical and Experimental Sonochemistry Involving Inorganic Systems, Springer Science & Business Media, Dordrecht, Heidelberg, London, New York, 2010, pp. 273–285.
[12] Pankaj, M. Chauhan, Sonochemical studies of aqueous solutions of chromium and manganese in their cationic and oxo-anionic states, Ind. J. Chem. 43A (2004) 1206–1209.
[13] L. Chen, Z. Chen, D. Chen, W. Xiong, Removal of hexavalent chromium from contaminated waters by ultrasound-assisted aqueous solution ball milling, J. Environ. Sci. 52 (2017) 276–283.
[14] M.N. Kathiravan, K. Muthukumar, Ultrasound mediated reduction of Cr(VI) using sludge obtained during electrocoagulation, Environ. Technol. 32 (2011) 1523–1531.
[15] O. Ayyildiz, E. Acar, B. Ileri, Sonocatalytic reduction of hexavalent chromium by metallic magnesium particles, Water Air Soil Pollut. 227 (2016) 363.
[16] N. Arul Dhas, Y. Koltypin, A. Gedanken, Sonochemical preparation and characterization of ultrafine chromium oxide and manganese oxide powders, Chem. Mater. 9 (1997) 3159–3163.
[17] C. Sehgal, R.G. Sutherland, R.E. Verrall, Cavitation-induced oxidation of aerated aqueous Fe^{2+} solutions in the presence of aliphatic alcohols, J. Phys. Chem. 84 (1980) 2920–2922.
[18] A. Henglein, C. Kormann, Scavenging of OH radicals produced in the sonolysis of water, Int. J. Radiat. Biol. 48 (1985) 251–258.
[19] S.I. Nikitenko, Plasma formation during acoustic cavitation: toward a new paradigm for sonochemistry, Adv. Phys. Chem. 17 (2014), http://dx.doi.org/10.1155/2014/173878.
[20] S.I. Nikitenko, C. Le Naour, P. Moisy, Comparative study of sonochemical reactors with different geometry using thermal and chemical probes, Ultrason. Sonochem. 14 (2007) 330–336.
[21] J. Rooze, E.V. Rebrov, J.C. Schouten, J.T.F. Keurentjes, Effect of resonance frequency, power input, and saturation gas type on the oxidation efficiency of an ultrasound horn, Ultrason. Sonochem. 18 (2011) 209–215.
[22] G. Mark, A. Tauber, R. Laupert, H.-P. Schuchmann, D. Schultz, A. Mues, C. von Sonntag, OH-radical formation by ultrasound in aqueous solution – Part II: terephthalate and Fricke dosimetry and the influence of various conditions on the sonolytic yield, Ultrason. Sonochem. 5 (1998) 41–52.
[23] A.O. Allen, C.J. Hochanadel, J.A. Ghormley, T.W. Davi, Decomposition of water and aqueous solutions under mixed fast neutron and gamma radiation, J. Phys. Chem. 56 (1952) 575–586.
[24] ASTM Standards D 1687-92, 1999.
[25] C. Wei, S. German, S.R. Basak, K. Rajeshwar, Photocatalytic reduction and immobilization of hexavalent chromium at titanium dioxide in aqueous basic media, J. Electrochem. Soc. 140 (1993) 2477–2482.
[26] J.M. Meichtry, M. Brusa, G. Mailhot, M.A. Grela, M.I. Litter, Heterogeneous photocatalysis of Cr(VI) in the presence of citric acid over TiO_2 particles: relevance of Cr(V)–citrate complexes, Appl. Catal. B 71 (2007) 101–107.
[27] J.J. Testa, M.A. Grela, M.I. Litter, Experimental evidence in favor of an initial one-electron-transfer process in the heterogeneous photocatalytic reduction of chromium(VI) over TiO_2, Langmuir 17 (2001) 3515–3517.
[28] J.J. Testa, M.A. Grela, M.I. Litter, Heterogeneous photocatalytic reduction of chromium(VI) over TiO_2 particles in the presence of oxalate. Involvement of Cr(V) species, Environ. Sci. Technol. 38 (2004) 1589–1594.
[29] J.M. Meichtry, C. Colbeau-Justin, G. Custo, M.I. Litter, Preservation of the photocatalytic activity of TiO_2 by EDTA in the reductive transformation of Cr(VI): studies by time resolved microwave conductivity, Catal. Today 224 (2014) 236–243.
[30] D.R. Lide (Ed.), CRC Handbook of Chemistry and Physics, 84th ed, CRC Press, Boca Raton, 2003–2004.
[31] X. Zhang, L. Song, X. Zeng, M. Li, Effects of electron donors on the TiO_2 photocatalytic reduction of heavy metal ions under visible light, Energy Proc. 17 (2012) 422–428.
[32] R. Sander, Compilation of Henry's law constants (version 4.0) for water as solvent, Atmos. Chem. Phys. 15 (2015) 4399–4981.
[33] M. Krumpolc, J. Roček, Stable chromium(V) compounds, J. Am. Chem. Soc. 98 (1976) 872–873.
[34] G. Mailhot, J.F. Pilichowski, M. Bolte, Unexpected dihydroxylation of methacrylamide photoinduced by chromium-(VI) in aqueous solution, New J. Chem. 19 (1995) 91–97.
[35] I.J. Buerge, S.J. Hug, Kinetics and pH dependence of chromium(VI) reduction by iron(II), Environ. Sci. Technol. 31 (1997) 1426–1432.
[36] A.E. Alegria, Y. Lion, T. Kondo, P. Riesz, Sonolysis of aqueous surfactant solutions. Probing the interfacial region of cavitation bubbles by spin trapping, J. Phys. Chem. 93 (1989) 4908–4913.
[37] E.L. Mead, R.G. Sutherland, R.E. Verrall, The effect of ultrasound on water in the presence of dissolved gases, Can. J. Chem. 54 (1976) 1114–1120.
[38] R. Pflieger, T. Chave, G. Vite, L. Jouve, S.I. Nikitenko, Effect of operational conditions on sonoluminescence and kinetics of H_2O_2 formation during the sonolysis of water in the presence of Ar/O_2 gas mixture, Ultrason. Sonochem. 26 (2015) 169–175.
[39] A. Henglein, Sonochemistry; historical developments and modern aspects, Ultrasonics 25 (1987) 6–16.
[40] M. Del Duca, E. Yeager, M.O. Davies, F. Hovorka, Isotopic techniques in the study of the sonochemical formation of hydrogen peroxide, J. Acoust. Soc. Am. 30 (1958) 301–307.
[41] R. Pflieger, H.P. Brau, S.I. Nikitenko, Sonoluminescence from $OH(C^2\Sigma^+)$ and $OH(A^2\Sigma^+)$ radicals in water: evidence for plasma formation during multibubble

cavitation, Chem. Eur. J. 16 (2010) 11801–11803.
[42] S.I. Nikitenko, R. Pflieger, Toward a new paradigm for sonochemistry: short review on nonequilibrium plasma observations by means of MBSL spectroscopy in aqueous solutions, Ultrason. Sonochem. 35 (2017) 623–630.
[43] C.A. Wakeford, R. Blackburn, P.D. Lickiss, Effect of ionic strength on the acoustic generation of nitrite, nitrate and hydrogen peroxide, Ultrason. Sonochem. 6 (1999) (1999) 141–148.
[44] M. Gutiérrez, A. Henglein, J.K. Dohrmann, H atom reactions in the sonolysis of aqueous solutions, J. Phys. Chem. 91 (1987) 6687–6690.
[45] F. Grieser, Sonochemistry in colloidal systems, in: P.V. Kamat, D. Meisel (Eds.), Semiconductor Nanoclusters Studies in Surface Science and Catalysis, vol. 103(9), Elsevier Science B.V., 1996, pp. 57–77.
[46] K. Okitsu, Sonochemical synthesis of metal nanoparticles, in: Pankaj, M. Ashokkumar (Eds.), Theoretical and Experimental Sonochemistry Involving Inorganic Systems, Springer Science & Business Media, Dordrecht, Heidelberg, London, New York, 2010, pp. 131–150.
[47] D.A. Vander Griend, J.S. Golden, C.A. Arrington Jr., Kinetics and mechanism of chromate reduction with hydrogen peroxide in base, Inorg. Chem. 41 (2002) 7042–7048.
[48] M. Pettine, L. Campanella, F.J. Millero, Reduction of hexavalent chromium by H_2O_2 in acidic solutions, Environ. Sci. Technol. 36 (2002) 901–907.
[49] A.D. Bokare, W. Choi, Chromate-induced activation of hydrogen peroxide for oxidative degradation of aqueous organic pollutants, Environ. Sci. Technol. 44 (2010) 7232–7237.
[50] A.D. Bokare, W. Choi, Advanced oxidation process based on the Cr(III)/Cr(VI) redox cycle, Environ. Sci. Technol. 45 (2011) 9332–9338.
[51] W. van Niekerk, J.J. Pienaar, G. Lachmann, R. van Eldik, M. Hamza, A kinetic and mechanistic study of the chromium (VI) reduction by hydrogen peroxide in acidic aqueous solutions, Water SA 33 (2007) 619–626.
[52] J.Z. Sostaric, P. Mulvaney, F. Grieser, Sonochemical dissolution of MnO_2 colloids, J. Chem. Soc. Faraday Trans. 91 (1995) 2843–2846.
[53] A. Brotchie, F. Grieser, M. Ashokkumar, The role of salts in acoustic cavitation and the use of inorganic complexes as cavitation probes, in: R. Pankaj, M. Ashokkumar (Eds.), Theoretical and Experimental Sonochemistry Involving Inorganic Systems, Springer Science & Business Media, Dordrecht, Heidelberg, London, New York, 2010, pp. 357–379.
[54] K. Okitsu, M. Iwatani, K. Okano, Md. Helal Uddin, Rokuro Nishimura, Mechanism of sonochemical reduction of permanganate to manganese dioxide in aqueous alcohol solutions: reactivities of reducing species formed by alcohol sonolysis, Ultrason. Sonochem. 31 (2016) 456–462.
[55] M.R. Hoffmann, I. Hua, R. Höchemer, Application of ultrasonic irradiation for the degradation of chemical contaminants in water, Ultrason. Sonochem. 3 (1996) S163–S172.
[56] J.A. Frim, J.F. Rathman, L.K. Weavers, Sonochemical destruction of free and metal-binding ethylenediaminetetraacetic acid, Water Res. 37 (2003) 3155–3163.
[57] G.V. Buxton, C.L. Greenstock, W.P. Helman, A.B. Ross, Critical review of rate constants for reactions of hydrated electrons, hydrogen atoms and hydroxyl radicals ($^{\cdot}OH/^{\cdot}O^{-}$) in aqueous solution, J. Phys. Chem. Ref. Data 17 (1988) 513–886.
[58] Z. Wang, R.T. Bush, L.A. Sullivan, J. Liu, Simultaneous redox conversion of chromium(VI) and arsenic(III) under acidic conditions, Environ. Sci. Technol. 47 (2013) 6486–6492.
[59] P. Romo-Rodríguez, F.J. Acevedo-Aguilar, A. Lopez-Torres, K. Wrobel, K. Wrobel, J.F. Gutiérrez-Corona, Cr(VI) reduction by gluconolactone and hydrogen peroxide, the reaction products of fungal glucose oxidase: cooperative interaction with organic acids in the biotransformation of Cr(VI), Chemosphere 134 (2015) 563–570.
[60] R. Kidak, N.H. Ince, Ultrasonic destruction of phenol and substituted phenols: a review of current research, Ultrason. Sonochem. 13 (2006) 195–199.
[61] T. Sivasankar, V.S. Moholkar, Mechanistic approach to intensification of sonochemical degradation of phenol, Chem. Eng. J. 149 (2009) 57–69.
[62] J.C. Sullivan, J.E. French, A kinetic study of the reaction between chromium(VI) and hydroquinone, J. Am. Chem. Soc. 87 (1965) 5380–5382.
[63] D.I. Pattison, M.J. Davies, A. Levina, N.E. Dixon, P.A. Lay, Chromium(VI) reduction by catechol(amine)s results in DNA cleavage in vitro: relevance to chromium genotoxicity, Chem. Res. Toxicol. 14 (2001) 500–510.
[64] M. Gutierrez, A. Henglein, C.-H. Fischer, Hot spot kinetics of the sonolysis of aqueous acetate solutions, Int. J. Radiat. Biol. 50 (1986) 313–321.
[65] A. Tauber, G. Mark, H.-P. Schuchmann, C. von Sonntag, Sonolysis of tert-butyl alcohol in aqueous solution, J. Chem. Soc. Perkin Trans. 2 (1999) 1129–1135.
[66] M. Breitenkamp, A. Henglein, J. Lilie, Mechanism of the reduction of lead ions in aqueous solution (a pulse radiolysis study), Ber. Bunsenges. Phys. Chem. 80 (1976) 973–979.
[67] R. Pflieger, A.A. Ndiaye, T. Chave, S.I. Nikitenko, Influence of ultrasonic frequency on swan band sonoluminescence and sonochemical activity in aqueous tert-butyl alcohol solutions, J. Phys. Chem. B 119 (2015) 284–290.
[68] D.Y. Chung, H.-i. Kim, Y.-H. Chung, M.J. Lee, S.J. Yoo, A.D. Bokare, W. Choi, Y.-E. Sung, Inhibition of CO poisoning on Pt catalyst coupled with the reduction of toxic hexavalent chromium in a dual-functional fuel cell, Sci. Rep. 4 (2014), http://dx.doi.org/10.1038/srep07450 Article number 7450.
[69] E.J. Hart, A. Henglein, Sonolysis of formic acid-water mixtures, Radiat. Phys. Chem. 32 (1988) 11–13.
[70] P.J. Wardman, Reduction potentials of one-electron couples involving free radicals in aqueous solution, J. Phys. Chem. Ref. Data 18 (1989) 1637–1755.
[71] H. Destaillats, H.M. Hung, M.R. Hoffmann, Degradation of alkylphenol ethoxylate surfactants in water with ultrasonic irradiation, Environ. Sci. Technol. 34 (2000) 311–317.
[72] J.Z. Sostaric, P. Riesz, Sonochemistry of surfactants in aqueous solutions: an EPR spin-trapping study, J. Am. Chem. Soc. 123 (2001) 11010–11019.
[73] H. Destaillats, T.W. Alderson II, M.R. Hoffmann, Applications of ultrasound in NAPL remediation. Sonochemical degradation of TCE in aqueous surfactant solutions, Environ. Sci. Technol. 35 (2001) 3019–3024.
[74] E.J. Hart, A. Henglein, Free radical and free atom reactions in the sonolysis of aqueous iodide and formate solutions, J. Phys. Chem. 89 (20) (1985) 4342–4347.
[75] P. Lukes, E. Dolezalova, I. Sisrova, M. Clupek, Aqueous-phase chemistry and bactericidal effects from an air discharge plasma in contact with water: evidence for the formation of peroxynitrite through a pseudo-second-order post-discharge reaction of H_2O_2 and HNO_2, Plasma Sources Sci. Technol. 23 (2014) 015019.
[76] B.P. Vellanki, B. Batchelor, A. Abdel-Wahab, Advanced reduction processes: a new class of treatment processes, Environ. Eng. Sci. 30 (2013) 264–271.
[77] Z. Luo, N. Chatterjee, Kinetics of oxidation of Cr(III)-organic complexes by H_2O_2, Chem. Spec. Bioavail. 22 (2010) 25–34.